

## GALACTIC CHEMICAL EVOLUTION WITH NEARLY CONSTANT STAR-FORMATION RATES

SARBANI BASU

Tata Institute of Fundamental Research, Homi Bhabha Road, Bombay 400 005, India

AND

N. C. RANA

Inter-University Centre for Astronomy and Astrophysics, Post Bag No. 4, Ganeshkhind, Pune 411 007, India

*Received 1993 January 25; accepted 1993 May 3*

## ABSTRACT

In this work we have investigated a set of closed models of Galactic chemical evolution with nearly constant star-formation rates. The star-formation rates ( $\psi$ ) we have considered depend both on the surface density of gas and the metallicity, and are of the form  $\psi \propto \Sigma_g^\alpha Z^\beta$ . In Rana & Basu (1992) we showed how such a form can probably be used to model the solar neighborhood and reproduce the age-metallicity relation (AMR) which had been derived from the observational age and metallicity distribution of stars. A more detailed investigation is reported here. We have first modeled the solar neighborhood and then extended the results to the rest of the Galaxy. One novel feature of this investigation is that the initial mass function (IMF) used for each model with a set of  $(\alpha, \beta)$  is calculated from the observed present-day mass function of main-sequence stars in the solar neighborhood and using the star-formation rate corresponding to that model. The different parameters of the model, such as the present rate of star formation at the solar neighborhood  $(\psi_1)_\odot$ , the returned gas fraction,  $R$ , and the total surface mass density,  $\Sigma_{\text{tot}}$  are calculated from the initial mass function and hence are not free parameters. We find that the parameter range  $\alpha = 1.15 \pm 0.05$ ,  $\beta = 1.25 \pm 0.05$  fits various observational data of the solar neighborhood better than the parameter range used in our previous work. The resulting model is such that the yield of iron,  $y$ , obtained from the model is consistent with that calculated from the IMF. The fit to the Galactic data is reasonable. We find that the fit to the data on Galactic radial variations improves if it is further assumed that the efficiency of star formation varies across the face of the Galaxy by about 10%. We also find that the resultant star-formation rate per unit area of the disk is consistent with one which is proportional to some power of the surface mass density of molecular hydrogen.

*Subject headings:* Galaxy: abundances — Galaxy: evolution — Galaxy: stellar content — stars: formation

## 1. INTRODUCTION

The history of the star-formation rate (SFR) has till recently been known only indirectly. There has been growing evidence that the star-formation rate in the solar neighborhood has remained more or less unchanged. The first results were based on arguments of continuity of the initial mass function (IMF); Miller & Scalo (1979) argued that the past average stellar birthrate should be between 0.4 to 3 times the present birthrate. Twarog (1980) analyzed a sample of F stars, and determined their ages using theoretical isochrones, and concluded that the ratio of the past average rate to the present SFR is less than 2.5, he, however, favored a value between 1 and 0.5. Carlberg et al. (1985) had similar conclusions. From studies of the white dwarf luminosity function, Rana (1990) also found that the data were best explained if the SFR is nearly constant.

There have recently been some direct determinations of the evolution of the SFR in the solar neighborhood. Soderblom, Duncan, & Johnson (1991) found the chromospheric ages of a reasonably volume-limited sample of stars and said that the cumulative age distribution of the stars was consistent with a constant star-formation rate. Rana & Basu (1992, hereafter Paper I) demonstrated that if the sample is corrected for the effects of disk heating assuming an isothermal disk (Amendt & Cuddeford 1991), and the vertical scale-height parameterization of Villumsen (1985), the sample is even more consistent with a nearly constant SFR. However, the sample is more consistent with a star-formation rate with a broad peak between 6 and 9 Gyr than with a totally flat SFR. This

becomes clear if the stars are binned in somewhat wider bins to reduce the effects of having a small sample of data.

In Paper I, we derived the age-metallicity relation at the solar neighborhood using the metallicity distribution of stars given by Pagel (1989) and the age distribution given by Soderblom et al. (1991). We also showed that the AMR could be reproduced if the star-formation rate depends on both the surface density of gas and the metallicity, and was nearly constant. In the present work, we have further investigated the consequences of using nearly constant star formation rates. We have extended our goal to see if we can reproduce not just the AMR and the SFR history, but also the G dwarf metallicity distribution and rate of formation of white dwarfs in the solar neighborhood. Besides, we have tried to apply the model to the rest of the Galactic disk as well.

We have considered closed models with no vertical infall of gas into the system, nor have we considered any gas flows in the radial direction. The models have first been constrained using solar neighborhood data and then applied uniformly to fit the rest of the Galactic disk. In § 2 we discuss the observational constraints on the models. Section 3 describes the models and the method followed in constraining them. The results are discussed in § 4, and in § 5 we state our conclusions.

## 2. OBSERVATIONAL CONSTRAINTS

The solar neighborhood observations we have considered are the evolution of star formation rate, the G dwarf metallicity

distribution curve, the age-metallicity relation, and ratio between the current rates of various types of supernovae.

The constraints on the evolution of SFR have already been mentioned in the preceding section. Since the Soderblom et al. (1991) data sample on SFR contains stars with ages of up to 13 Gyr, we consider the age of the Galactic disk,  $t_d$ , to be 13 Gyr.

The second important constraint is the metallicity distribution, or more correctly the iron-abundance distribution of G dwarfs in the solar neighborhood. We use the distribution of Pagel (1989). We have used his "uncorrected" sample, since we have corrected for the possible intrinsic scatter and the observational errors ourselves by convolving the predicted curve with a Gaussian with  $\sigma = 0.2$  dex, the same mean error as adopted by Pagel (1989).

As far as the age-metallicity relation is concerned, in addition to the AMR derived in Paper I, we have considered the AMRs determined by Twarog (1980), Carlberg et al. (1985), Meusinger, Reimann, & Stecklum (1991), Nissen, Edvardsson, & Gustafsson (1985), and Strobel (1991). The AMRs of the first three groups are derived from photometric data of the same sample of stars. The differences arise due to the final selected sample of stars, and the different isochrones used. That of Nissen et al. (1985) was derived from a sample of stars with spectroscopically determined abundances, and the AMR of Strobel (1991) has been derived from open cluster data. Since the use of different isochrones have resulted in a different total disk age for each of the AMRs, all these relations have been duly normalized to the adopted disk age of 13 Gyr.

The current average metallicity at the solar neighborhood is taken to be  $[\text{Fe}/\text{H}] = 0.12$  dex, which is the metallicity of the Hyades cluster and supposed to be the representative metallicity of the local ISM within 0.5 kpc of the Sun (Nissen 1988). The G dwarf sample of Pagel (1989) contains stars with a metallicity up to  $[\text{Fe}/\text{H}] = 0.20$  dex, while other samples (for example, Sommer-Larsen 1991) have stars even up to  $[\text{Fe}/\text{H}] = 0.40$  dex. With an assumed present-day average metallicity of  $[\text{Fe}/\text{H}] = 0.12$  dex for stars in the solar neighborhood, the scatter considered can account for the presence of the higher metallicity stars.

There seems to be a wide variation in the determined rates of supernovae. The estimated rates of Type II supernovae vary from  $0.010 \text{ pc}^{-2} \text{ Gyr}^{-1}$  (van den Bergh, McClure, & Evans 1987) to  $0.031 \text{ pc}^{-2} \text{ Gyr}^{-1}$  (Narayan 1986). For the ratios of the rates of the various types of supernovae, we have adopted the Evans, van den Bergh, & McClure (1989) result of 1.04:0.28:0.27 for supernovae of Type II (SN II), Type Ia (SN Ia), and Type Ib (SN Ib), respectively. This agrees with the ratios mentioned in van den Bergh & Tamman (1991).

The Galactic constraints include the radial variation of the surface mass density of gas, metallicity, and the present-star formation rates in the disk. We have used the radial variation of the surface density of molecular hydrogen as a supplementary constraint. We have taken molecular hydrogen mass estimates from Bhat et al. (1985) and Bronfman et al. (1988). Atomic hydrogen data are from Burton & Gordon (1978) and Deul (1988). We have assumed that hydrogen constitutes 70% by mass of the gas present. This means that the surface mass density of gas at the solar neighborhood (at 8.5 kpc from the Galactic center) is  $(\Sigma_{g1})_{\odot} = 6.6 \pm 2.5 M_{\odot} \text{ pc}^{-2}$ , where the uncertainty is mainly due to the uncertainty in the conversion factor from CO emissivities to molecular hydrogen mass.

Data on the distribution and gradient of the abundance of iron in the Galaxy have been obtained from Janes (1979), Luck (1982), and Cameron (1985). For each sample we have deter-

mined  $Z_R$ , the metallicity in the solar neighborhood, and normalized the rest of the data to this value. This can to some extent correct for the differences in the zero-point in the metallicity calibration, and the fact that the samples contain objects with mixed ages.

The radial variation of SFR is taken from Lacey & Fall (1985), which includes data from Mezger (1978) for SFR determinations using  $\text{H}\alpha$  emission, Lyne, Manchester, & Taylor (1985) for SFR from pulsar birthrate data, and Guibert, Lequeux, & Viallefond (1978) for SFR determinations using the distribution of supernova remnants. In all cases the SFR has been normalized, with the SFR at the solar neighborhood taken as unity. This avoids the error which is introduced by the use of any particular mass function while converting the SFR at the high-mass end, which is the quantity actually observed, into the total SFR.

### 3. THE MODELS

We have constructed closed models of the Galaxy. This means that there is no infall of gas into the system nor outflow of gas from the system. Thus the total mass density of the system remains constant. This also means that other than by ejections from old stars, there is no way of replenishing the gas reservoir once the gas has been locked up in stars. Thus in closed models, a star-formation rate which depends only on the surface mass density of gas cannot give rise to a constant SFR. For the star-formation rate to remain almost constant over the age of the Galaxy it must depend on some quantity other than the gas content. This other quantity has to be an increasing function of time. The simplest parameterization which can give the required form is thus a SFR of the form used in Paper I,

$$\psi = a \Sigma_g^{\alpha} (Z/Z_{\odot})^{\beta}, \quad (1)$$

where  $\Sigma_g$  is the surface density of gas,  $Z$  is the metallicity, and  $a$  is the constant of proportionality. As the Galaxy evolves,  $\Sigma_g$  decreases as more and more gas is locked up into stars. But as stars evolve and die, they enrich the interstellar medium. Thus the metallicity  $Z$  increases with time, thereby offsetting the effects of a decreasing gas density in the SFR. No other reasonable form of the SFR gives nearly constant star-formation rates for a closed model. This adopted form has been used by Rana & Wilkinson (1986, 1988) and Tosi & Diaz (1990). Both sets of authors use the abundance of oxygen for the value of  $Z$  and have kept the ratio  $(\alpha/\beta)$  constant at a value of 1.3 in order to maintain the observed relationship between the molecular hydrogen fraction and the abundance of oxygen. We have relaxed this condition and have searched the two-dimensional parameter space of  $\alpha$  and  $\beta$  in order to see if any set of  $\alpha$  and  $\beta$  can reproduce the observed features of the solar neighborhood and the Galaxy when the abundance of iron rather than oxygen is considered. We test later if the selected SFR has any correlation with the fraction of molecular hydrogen. We have used the abundance of iron as  $Z$  since all relevant observations (AMR, G-Dwarf metallicity distribution function, supernova yields, etc.) are known better, or sometimes exclusively, in terms of the abundance of iron normalized to the solar photospheric abundance of iron.

We have used the instantaneous recycling approximation (IRA). This involves the assumption that stars are of two categories. The high-mass stars, which have very short lifetimes compared to the lifetime of the Galaxy, and hence can be assumed to die as soon as they are born enriching the inter-

stellar medium instantaneously. The other category consists of long-lived low-mass stars. These stars do not die during the lifetime of the Galaxy, thus they do not enrich the interstellar medium, but only lock up gas. In § 4.9 we discuss the effects of relaxing IRA. In Table 1 we list the abbreviations used and their definitions.

The constant of proportionality  $a$  in equation (1), is not a free parameter of the models. It is determined uniquely for each set of parameters,  $(\alpha, \beta)$ , from the initial mass function (IMF) of stars in the solar neighborhood.

In this work we consider the observed present-day mass function (PDMF) and not the IMF of stars to be a fundamental function. The calculation of the IMF from the observed PDMF of stars requires the knowledge of the history of star formation (see Miller & Scalo 1979; Scalo 1986; Rana 1987; Basu & Rana 1992). Thus the IMF for each of the SFRs would be different. We have calculated the IMF for each SFR in the manner described in Basu & Rana (1992), which takes into account the multiplicity of stars in the solar neighborhood. The IMF has to be calculated iteratively. An SFR of the form given in equation (1) is only an implicit function of time. To obtain the actual time variation of the SFR, the equations of chemical evolution have to be solved, which in turn would depend on quantities calculated from the IMF. Hence the process of iteration becomes a necessity.

The IMF is generally defined as a function representing the number of stars ever formed per unit area of the disk per unit logarithmic interval of stellar mass (see Miller & Scalo 1979). Thus if  $\xi(\log m)$  be the IMF, then (see Rana 1987)

$$\int_{m_l}^{m_u} \xi(\log m) d \log m = \int_0^{t_d} \psi(t) dt, \quad (2)$$

where  $m_l$  and  $m_u$  are, respectively, the lower and upper limits to the mass of stars formed. The left-hand side of the equation can be calculated from the IMF. For this we have considered a lower mass limit of  $0.08 M_\odot$ . We have kept the upper mass limit at  $100 M_\odot$ . However, since the IMF is very steep at the high-mass range the integral is not very sensitive to the upper limit, for example, if the IMF is calculated for an absolutely constant SFR, the integral changes from  $54.21 M_\odot \text{ pc}^{-2}$  for  $m_u = 50 M_\odot$  to  $54.76 M_\odot \text{ pc}^{-2}$  for  $m_u = 100 M_\odot$ . Once we know the relative SFR, the right-hand side of equation (2) can be calculated and hence the constant of proportionality,  $a$ , determined. Thus for a given set of parameters,  $(\alpha, \beta)$  the SFR is determined completely, and there is no freedom left to adjust the scale of star formation. One point to note however is that

this star-formation rate will not include the rate of formation of brown dwarfs, since the lower mass limit of the observed IMF in the present work extends only down to  $0.08 M_\odot$ .

Another factor which we calculate from the IMF is the returned fraction of gas,  $R$ . The yield,  $y$ , too can in principle, be calculated directly from the IMF. However, to calculate the yield, we only estimate the total surface mass density of the disk (see Basu & Rana 1992) in the solar neighborhood. The yield is then calculated using the standard formula for a closed model (Tinsley 1980):

$$y = \frac{Z_1 - Z_0}{\ln(\mu_0/\mu_1)}, \quad (3)$$

where  $Z_1$  is the metallicity today,  $Z_0$  is the initial disk metallicity, and  $\mu_0$  and  $\mu_1$  are the initial and final gas fractions, respectively. Thus once the two powers  $\alpha$  and  $\beta$  are decided, all other parameters of the model are determined completely in a totally self-consistent manner.

We also try to determine the mass range of supernova progenitors which can match the value of the yield of iron calculated from equation (3). Since we deal with SFRs which have remained nearly constant over the age of the Galaxy, we can assume that the past average ratio of the rate of the different types of supernovae is equal to the present ratio of their rates. The nucleosynthesis prescriptions we use is as follows: we assume that supernovae of Type II produce  $0.075 M_\odot$  of iron, but those with a progenitor mass below  $12 M_\odot$  do not produce any iron at all (Nomoto, Shigeyama, & Tsujimoto 1990). The progenitor mass range of a Type Ib supernova is thought to be from  $12$  to  $20 M_\odot$ , and they eject around  $0.15 M_\odot$  of iron (Nomoto et al. 1990). A supernovae of Type Ia produces about  $0.6 M_\odot$  of iron (Nomoto, Thielmann, & Yokoi 1984). Type Ia supernovae are assumed to be produced in binaries. The progenitor mass is assumed to be between  $3 M_\odot$  and the lower limit of the SN II progenitor mass range.

Once the SN II mass range is fixed, the number of SN II's that have exploded can be calculated from the IMF, and using the observed ratio of the rates of supernovae of different types, we can calculate the number of the other types of supernovae, and hence calculate the total semi-theoretical yield of iron. Thus by varying the mass range of SN II progenitors we can find out which mass range of SN II progenitors gives the value of  $y(1 - R)$  consistent with that calculated from equation (1).

It is generally believed that SN II explosions occur in stars which were initially more massive than  $8 M_\odot$  (Nomoto 1984; Branch 1984). However, Becker & Iben (1980) put this limit

TABLE 1  
ABBREVIATIONS USED

Abbreviation	Expansion	Definition
SFR .....	Star-formation rate	The mass of stars formed per unit time per unit area.
AMR .....	Age-metallicity relation	The variation of metallicity with time. Observationally, it is the variation of iron abundance of the gas from which stars are formed with time.
PDMF .....	Present-day mass function	The number of stars present today per unit area of the Galactic disk, per unit logarithmic interval of stellar mass.
IMF .....	The initial mass function	The total number of stars ever formed per unit area of the of the Galactic disk, per unit logarithmic interval of stellar mass. The normalized IMF is the stellar mass spectrum at birth.
IRA .....	Instantaneous recycling approximation	The assumption that stars are of two categories: high-mass stars that die as soon as they are born enriching the interstellar medium instantaneously; and low-mass stars that live throughout the life of the Galaxy and serve only to lock up gas.

slightly higher at  $8.95 M_{\odot}$ . Maeder & Meynet (1989) claim that the inclusion of convective overshoot reduces this mass limit to  $6.6 M_{\odot}$ . On the other hand, there have also been suggestions that 8 to  $10 M_{\odot}$  stars can be progenitors of Type I supernovae (Woosley, Weaver, & Taam 1980). All authors seem to agree, though, that stars of mass greater than  $12 M_{\odot}$  form iron cores and give rise to SN II's. We, therefore, adopt 8 to  $12 M_{\odot}$  as the acceptable range within which the lower limit of the SN II progenitor mass should lie.

In order to overcome the G dwarf problem in a closed model such as ours, we have to postulate an initial metallicity at the time of formation of the Galactic disk. The form of SFR we have chosen also necessitates such an assumption. We find that an initial metallicity equivalent to  $[\text{Fe}/\text{H}] = -0.8$  dex to  $[\text{Fe}/\text{H}] = -0.9$  dex is sufficient to solve the G dwarf problem. For  $[\text{Fe}/\text{H}](t=0) > -0.8$  dex very few stars are formed in the low-mass range, while  $[\text{Fe}/\text{H}](t=0) < -0.9$  dex results in the G dwarf problem. We therefore, adopt an initial metallicity of  $[\text{Fe}/\text{H}] = -0.85$  dex.

The more metal poor, and hence older, stars in the G dwarf sample would have had their vertical scale heights enhanced due to effects of disk heating. Therefore, before comparing the theoretical G dwarf metallicity distribution curve with the observed one, we have weighted the predicted curve inversely by the factor by which the scale heights would have increased in the observed sample. The predicted curve was corrected instead of the observed one since the correction is model dependent, and correcting the sample would result in a different distribution for each model, making comparisons difficult. To take care of the effects of possible intrinsic scatter and observational error in the sample, we have convolved each curve with a Gaussian with  $\sigma = 0.2$  dex, which is the spread in metallicity assumed in the G dwarf sample of Pagel (1989).

In extending the models to the rest of the disk of the Galaxy, we have assumed that the IMF for the solar neighborhood holds everywhere; thus quantities like the returned fraction and yield will be constant across the face of the Galaxy. We

have calculated the final surface mass density of gas,  $\Sigma_g$ , final metallicity,  $Z_1$ , and star-formation rate  $\psi_1$ , in annuli, each of width 1 kpc, centered at the center of the Galaxy. We have calculated the initial gas mass  $\Sigma_{g0}$ , in each annulus by assuming that the Galactic disk has an exponential mass distribution with a radial scale length of 3.65 kpc (from Bahcall, Schmidt, & Soneira 1983). For normalization, the mass at the solar neighborhood, that is at  $R_G = 8.5$  kpc was calculated from the local IMF.

#### 4. RESULTS AND DISCUSSION

We have solved the equations for chemical evolution for a large number of models scanning a wide range of the parameter space covered by the two parameters  $\alpha$ , the exponent of the surface mass density of gas in the SFR, and  $\beta$ , the exponent of the metallicity. Some features which are conspicuous are as follows.

##### 4.1. The Star-Formation Rate

Figure 1 shows the variation of the SFR for different values of  $\alpha$  and  $\beta$ . For a given value of  $\alpha$ , the ratio of the past average SFR to the present SFR decreases with increasing  $\beta$ . The peak of the SFR shifts nearer the present epoch as the dependence on metallicity increases. Figure 1a shows the variation of the SFR when  $\beta$  is varied for a given  $\alpha$ , while Figure 1b shows the variation when  $\beta$  is held constant and  $\alpha$  is allowed to vary. As can be seen, the variation of the SFR rules out models in which the SFR depends on the surface mass density of gas only. In such cases, the SFR is a sharply decreasing function of time, and the time variation is nowhere near the observed one. For higher values of  $\beta$ , the SFRs match the observed distribution fairly well. However if  $\beta$  becomes very high, the peak shifts too much towards the present. Thus for  $\alpha = 1.15$ ,  $\beta$  in the range 1.0 to 1.3 seem to give a fairly good match to the observed SFR. For a given  $\beta$ , a decrease in  $\alpha$  pushes the peak toward the present. At  $\beta = 1.25$ , the acceptable values of  $\alpha$  range from 1.10 to 1.40.

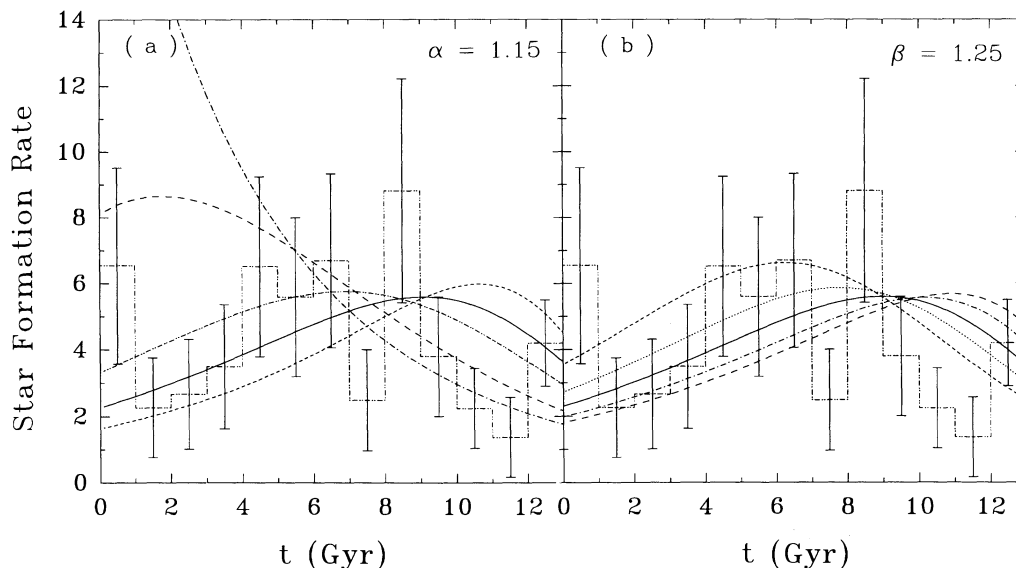


FIG. 1.—(a) History of the star-formation rate for  $\alpha$  kept constant at 1.15. The ordinate is in units of  $M_{\odot} \text{pc}^{-2} \text{Gyr}^{-1}$ . The dot-dashed line is the curve for the model with  $\beta = 0.0$ , the long dashes for  $\beta = 0.5$ , the chain dotted for  $\beta = 1.0$ , solid for  $\beta = 1.25$ , and medium dashes for  $\beta = 1.5$ . (b) History of the SFR for models with  $\beta$  kept constant at 1.25. The curve with long dashes is for the model with  $\alpha = 0.90$ , the dot-dashed line for  $\alpha = 1.00$ , the solid line for  $\alpha = 1.15$ , the dotted line for  $\alpha = 1.30$ , and the medium dashed line for  $\alpha = 1.4$ . In both figures, the histogram in the background is the SFR as derived from the data of Soderblom et al. (1991).

#### 4.2. Importance of Considering a Consistent Initial Mass Function

The need to calculate the IMF for each SFR becomes very clear if one looks at Figure 2, which shows the variation of several quantities derived from the IMF. The IMF at any given stellar mass,  $m$ , is inversely proportional to the integral of the SFR between times  $t_d - \tau_m$  and  $t_d$  (see Rana 1987), where  $\tau_m$  is the main-sequence lifetime of a star of that mass. Thus a shift of the SFR peak toward the present epoch would imply a decrease, at the high mass end, in the total number of stars that have ever been born. This would mean that the number of evolved stars and remnants which go into the calculation of the total surface mass density of the Galactic disk decreases, i.e., the estimates for the total surface mass density will decrease. This in turn means an increase in the yield  $y$ , since the yield has an inverse relation with the total mass (eq. [3]). Again, a decrease in the number of high-mass stars would imply a decrease in the returned fraction  $R$  of gas. For a given  $\beta$ , the opposite trends would be seen if  $\alpha$  were to increase, since an increase in  $\alpha$  implies a shift in the SFR peak away from the present, and hence an increase in  $\langle \psi \rangle / \psi_1$ , the ratio of the past average SFR to the present. Figure 2a shows the variation of  $\langle \psi \rangle / \psi_1$  with  $\beta$  for various values of  $\alpha$ . In Figure 2b we show the variation of  $R$ , while Figure 2c shows the variation of  $y$ .

A more important fact is that a shift in the SFR peak toward the present epoch causes the value of  $y(1 - R)$  to increase. Since  $y(1 - R)$  is a measure of the actual fraction of new metals released (see Tinsley 1980), we can translate this quantity into the mass range of stars which become SN II, as has been discussed in § 3. Too high a value of  $y(1 - R)$  would mean that

the lower limit of SN II progenitor mass has to be lower than  $8 M_\odot$ , while if the quantity is very small, the lower mass limits has to be fairly high. Figure 2d shows the variation of  $y(1 - R)$  with  $\alpha$  and  $\beta$ . We find that for an increase in  $\alpha$ ,  $\beta$  has to be increased in order to keep the SN II progenitor mass limits within a suitable range.

#### 4.3. The Age-Metallicity Relation and the Metallicity Distribution

Figure 3 shows the AMR for various values of the parameters  $\alpha$  and  $\beta$ . For a given  $\alpha$ , changes in  $\beta$  seem to change the curvature of the predicted AMR. For very small  $\beta$  it is convex upward, becomes flatter as the value of  $\beta$  increases, and on further increase in  $\beta$  becomes concave upward. This behavior can be related to the time at which the peak of the SFR occurs. For small values of  $\beta$ , the SFR rises fast in the early phase of the history of the Galaxy. This causes an early rise in the metallicity, after which the metallicity growth slows down since the SFR drops, giving rise to a convex age-metallicity relation. On the other hand, if the peak in the SFR occurs very late, the growth of metallicity would be slow in the beginning, followed by rapid enrichment in the recent past.

The predicted G dwarf curves in general fit the observations quite well as can be seen from Figure 4. Therefore, we cannot use the predicted metallicity distribution to restrict any parameter other than the initial metallicity.

#### 4.4. The Supernova Progenitor Mass Range

In order to keep the lower limit of the mass of the progenitor of Type II supernovae in the range 7 to  $11 M_\odot$ , we find that

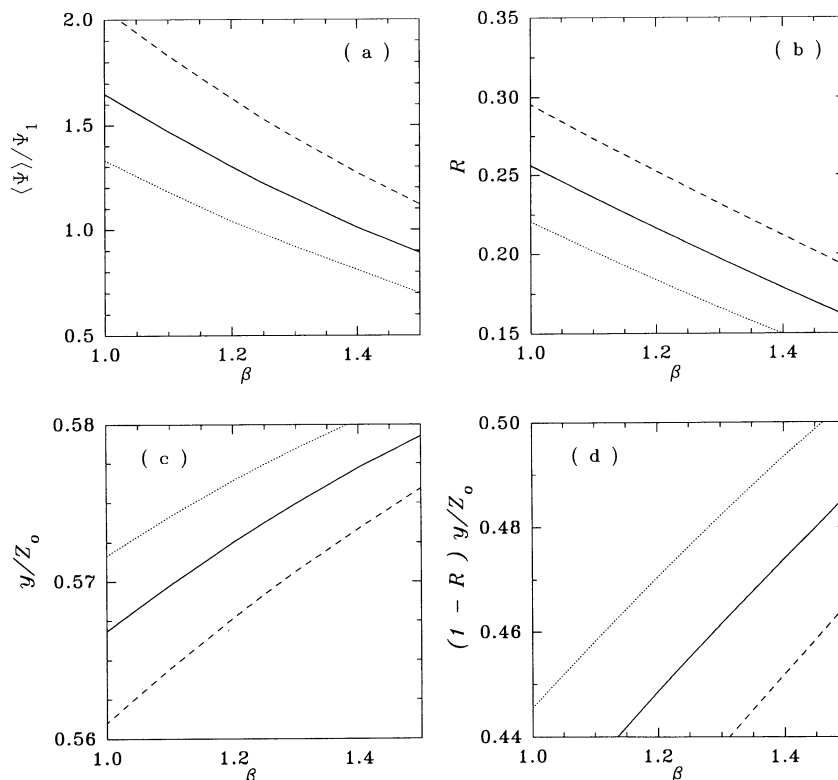


FIG. 2.—Various quantities derived from the star-formation rate and the corresponding IMF as a function of  $\beta$  for various  $\alpha$ . (a) Variation of the ratio of the past average star-formation rate to the present star-formation rate. (b) Returned fraction. (c) Yield in units of  $Z_\odot$ . (d) Product  $y(1 - R)$  in units of  $Z_\odot$ . In all figures, the dotted line is for  $\alpha = 1.00$ , the solid line is for  $\alpha = 1.15$ , and the dashed line is for  $\alpha = 1.30$ .

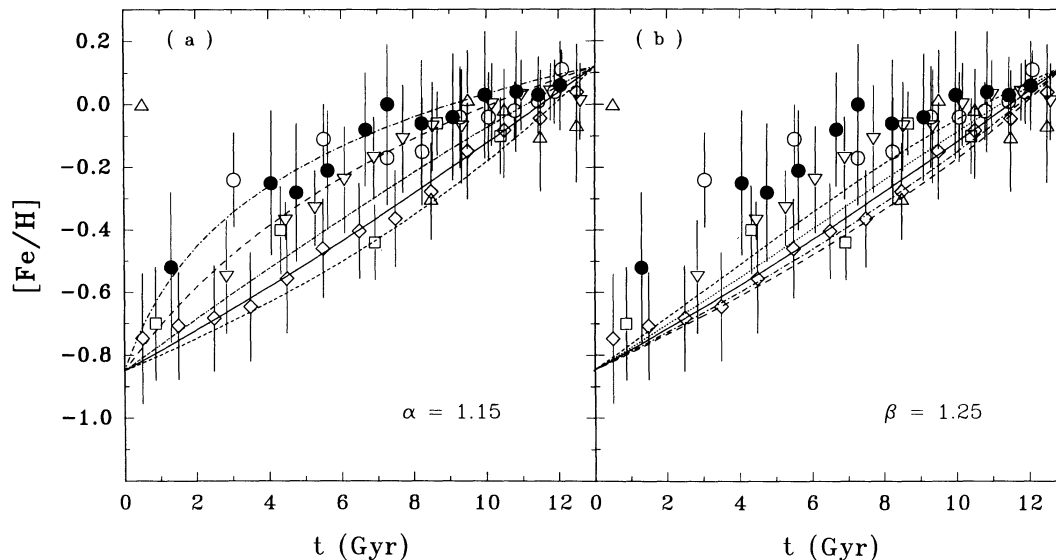


FIG. 3.—(a) Predicted AMR for various models with  $\alpha = 1.15$ . The different curves are for the same values of  $\beta$  as in Fig. 1a. (b) The predicted AMR for models with  $\beta = 1.25$ . The different types of curves correspond to the same  $\alpha$  values as is Fig. 1b. In both figures, the inverted triangles are data from Twarog (1980), the open circles are from Carlberg et al. (1985), the squares from Nissen et al. (1985), the triangles from Strobel (1991), the filled circles are data from Meusinger et al. (1991), and the diamonds are from Rana & Basu (1992).

with increasing  $\alpha$ ,  $\beta$  has to be increased. For example we find that for  $\alpha = 1.00$ ,  $\beta = 1.00$  gives a lower limit of  $10 M_{\odot}$ , while  $\beta = 1.40$  gives a lower limit of less than  $8 M_{\odot}$ . On the other hand, with  $\alpha = 1.30$ , the lower mass limits to the SN II progenitor mass are  $12 M_{\odot}$  and  $10 M_{\odot}$  for  $\beta = 1.00$  and  $\beta = 1.40$ , respectively.

Table 2 lists some of the properties of the models. Column (1) is the parameter  $\beta$ , column (2) is the current SFR in units of  $M_{\odot} \text{pc}^{-2} \text{Gyr}^{-1}$ . Columns (3) and (4) list the returned fraction and the yield, respectively. Column (5) shows the estimated total mass density, ( $\Sigma_t = \Sigma_{g0}$ ). The ratio of the past average to the present SFR is listed in column (6), while column (7) shows the epoch at which the SFR peaks. Column (8) lists the metallicity gradient expressed in units of  $\text{dex kpc}^{-1}$ , and columns (9)

and (10) show the lower and upper limits to the SN II progenitor mass required in order to match the value of yield listed in column (4).

#### 4.5. The Galactic Constraints

Figures 5, 6, and 7 show the predictions of selected models for the radial distributions of gas, metallicity ( $[\text{Fe}/\text{H}]$ ), and the present star-formation rate. The distributions of gas and metallicity in effect determine that of the SFR. We find that this set of data can constrain the parameters more effectively than the solar neighborhood data alone can.

If we consider the radial distribution of gas, we find that no set of parameters ( $\alpha$ ,  $\beta$ ), is able to reproduce the rise and fall of the gas distribution with the peak at about  $R_G = 5 \text{ kpc}$ . For

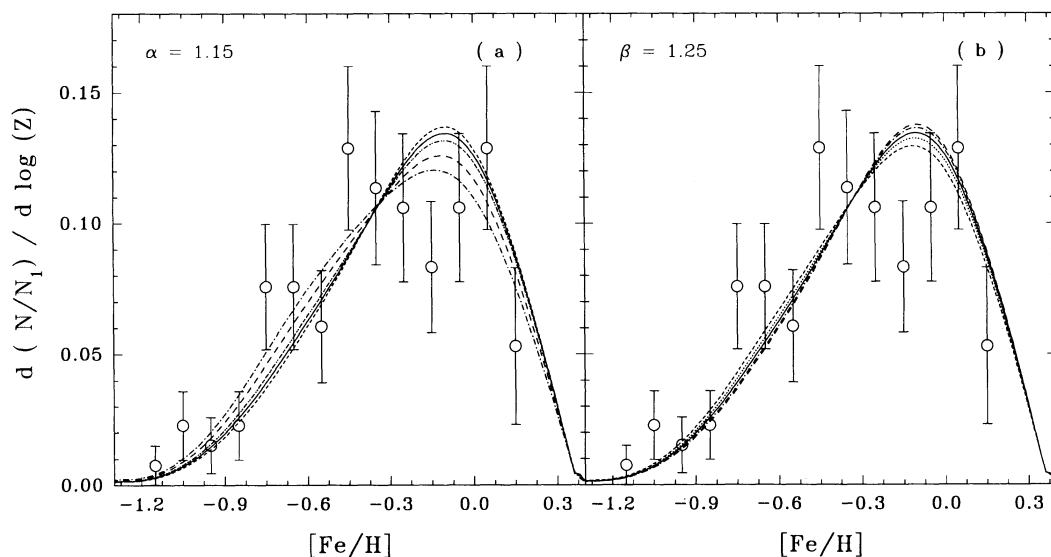


FIG. 4.—Predicted metallicity distribution of stars for (a) models with  $\alpha = 1.15$ , and (b) models with  $\beta = 1.25$ . The various curves are for the same parameters as mentioned in Fig. 1.

TABLE 2  
 PROPERTIES OF SOME MODELS

$\beta$ (1)	$(\psi_1)_\odot$ (2)	$R$ (3)	$y/Z_\odot$ (4)	$(\Sigma_{\text{tot}})_\odot$ (5)	$(\langle\psi\rangle/\psi_1)_\odot$ (6)	$t_{\psi(m)}$ (7)	$\frac{d \log Z/Z_R}{dR_G}$ (8)	$m_d$ (9)	$m_e$ (10)
$\alpha = 0.90$									
0.00.....	1.99	0.3826	0.5419	57.91	3.21	0.0	0.012	> 12.0	40
1.00.....	3.73	0.1987	0.5744	51.23	1.15	9.1	0.028	9.0	45
1.25.....	4.74	0.1558	0.5795	50.30	0.84	10.9	0.036	< 8.0	100
$\alpha = 1.00$									
1.00.....	3.35	0.2207	0.5716	51.73	1.33	8.1	0.000	10.0	40
1.10.....	3.66	0.2019	0.5741	51.27	1.18	9.0	0.000	9.5	85
1.25.....	4.20	0.1750	0.5774	50.67	0.98	10.2	0.000	8.0	40
1.30.....	4.41	0.1663	0.5785	50.49	0.92	10.5	0.000	8.0	85
1.50.....	5.46	0.1341	0.5820	49.87	0.70	11.6	0.000	< 8.0	40
$\alpha = 1.10$									
0.00.....	1.78	0.4305	0.5299	60.84	4.13	0.0	-0.010	> 12.0	< 40
1.10.....	3.28	0.2244	0.5713	51.79	1.36	8.2	-0.027	10.5	75
1.20.....	3.58	0.2052	0.5739	51.31	1.21	9.0	-0.030	9.5	55
1.25.....	3.75	0.1958	0.5751	51.10	1.14	9.4	-0.032	9.0	45
1.30.....	3.92	0.1865	0.5762	50.89	1.07	9.8	-0.035	8.5	40
1.50.....	4.80	0.1516	0.5802	50.17	0.82	11.0	-0.047	< 8.0	100
$\alpha = 1.15$									
0.00.....	1.73	0.4424	0.5265	61.72	4.40	0.0	-0.013	> 12.0	< 40
0.50.....	2.12	0.3556	0.5488	56.35	2.80	1.7	-0.020	> 12.0	< 40
1.00.....	2.89	0.2562	0.5668	52.64	1.65	6.8	-0.033	11.5	45
1.20.....	3.39	0.2165	0.5725	51.57	1.30	8.6	-0.042	10.0	55
1.25.....	3.54	0.2068	0.5738	51.34	1.22	9.0	-0.045	9.5	50
1.30.....	3.71	0.1973	0.5750	51.12	1.15	9.4	-0.048	9.0	45
1.50.....	4.51	0.1611	0.5792	50.35	0.89	10.6	-0.065	< 8.0	100
$\alpha = 1.20$									
1.00.....	2.75	0.2687	0.5650	53.00	1.77	6.4	-0.041	12.0	45
1.20.....	3.22	0.2282	0.5710	51.85	1.40	8.2	-0.051	10.5	55
1.25.....	3.36	0.2182	0.5724	51.60	1.32	8.6	-0.055	10.0	50
1.30.....	3.51	0.2084	0.5736	51.36	1.24	9.0	-0.058	9.5	45
1.50.....	4.24	0.1710	0.5782	50.53	0.96	10.3	-0.077	8.0	45
$\alpha = 1.30$									
1.00.....	2.51	0.2955	0.5610	53.79	2.05	5.6	-0.051	> 12.0	40
1.20.....	2.91	0.2526	0.5677	52.49	1.63	7.4	-0.063	11.5	50
1.25.....	3.02	0.2423	0.5692	52.19	1.53	7.8	-0.066	11.5	80
1.30.....	3.15	0.2320	0.5707	51.91	1.44	8.2	-0.070	11.0	85
1.50.....	3.77	0.1921	0.5759	50.95	1.12	9.7	-0.089	9.0	55
$\alpha = 1.40$									
1.25.....	2.74	0.2677	0.5656	52.88	1.76	7.0	-0.071	12.0	60
$\alpha = 1.50$									
1.25.....	2.49	0.2945	0.5615	53.70	2.06	6.3	-0.073	> 12.0	40

small values of  $\beta$  at a given value of  $\alpha$ , the gas distribution shows a continuous rise toward the center of the Galaxy. For large values of  $\beta$ , the gas distribution falls towards the center. There does exist an optimum range, but the fit is not very good, and does not quite reproduce the shape of the observed gas distribution. Of course one must remember that of all the observational quantities, the gas distribution is still the most controversial one.

The choice of parameters becomes a more difficult task if we try to reproduce the data on the metallicity gradient also. The metallicity gradient is an increasing function of  $\alpha$ , and for a given  $\alpha$ , it is an increasing function of  $\beta$ . However, as  $\alpha$

increases, the predicted amount of gas toward the center decreases, increase in  $\beta$  has similar effect. The gas distribution and the metallicity gradient in effect work in opposite directions when it comes to constraining the dependence of the star-formation rate on gas and metallicity. If we look for a good fit to the metallicity gradient, the fit to the gas distribution becomes bad.

As far as the radial distribution of the SFR is concerned, its behavior is dominated by that of the gas distribution. We see once again that no set of parameters,  $(\alpha, \beta)$ , can produce the sharp rise and subsequent fall of the spatial variation of the SFR.

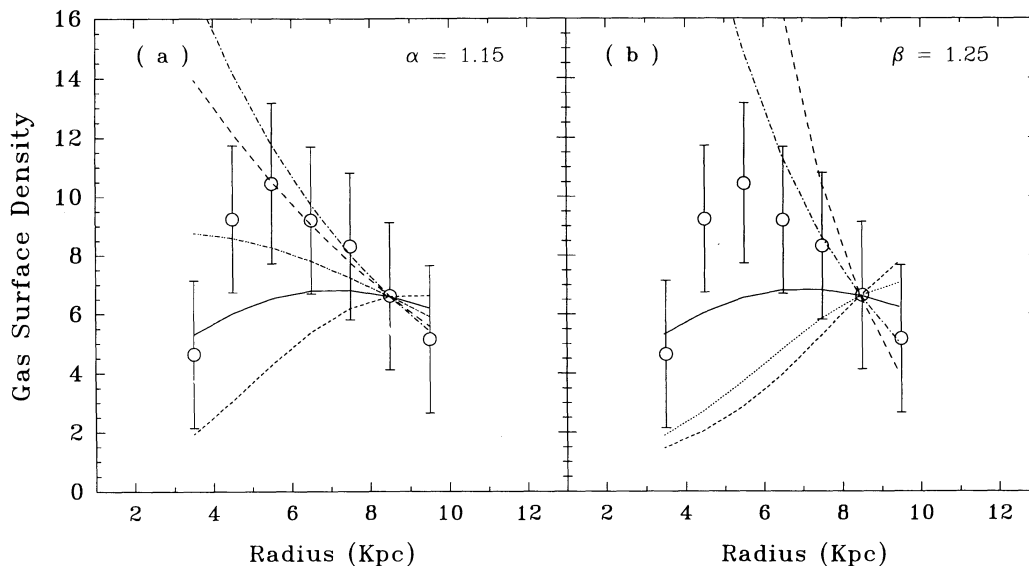


FIG. 5.—Radial distribution of the surface mass density of gas for (a) models with  $\alpha = 1.15$  and different values of  $\beta$  as in Fig. 1a, and (b) models with  $\beta = 1.25$ . The various types of lines correspond to the same values of  $\alpha$  as in Fig. 1b. The ordinate is in units of  $M_{\odot} \text{pc}^{-2}$ .

#### 4.6. Can the Parameters, $(\alpha, \beta)$ , Be Constrained at All?

The question we ask now is that knowing the predictions of the various models, can some constraint be put on the allowed parameter space of  $\alpha$ , and  $\beta$ ? Models with  $\alpha < 1.00$  are ruled out since they produce positive metallicity gradients. Any model with  $\alpha = 1.00$  is ruled out since it fails to produce any gradient in the metallicity at all. For  $\alpha \geq 1.20$ , the gas distribution shows a trend opposite that observed. The predicted amount of gas falls toward the center of the Galaxy, except for small  $\beta$ , which in any case have to be rejected because the SFR would then peak too early in the history of the evolution of Galaxy, and the lower limit to the mass of the progenitors of Type II supernovae would be unacceptably large. Therefore,

the acceptable value for  $\alpha$  seems to lie in the range  $\alpha = 1.15 \pm 0.05$ .

As for the dependence on metallicity,  $\beta$ , small values of  $\beta (< 1.2)$  can be rejected on three accounts. First, the SFR history at the solar neighborhood does not match; second, the calculated lower limit to the SN II progenitor mass is very large ( $\sim 12 M_{\odot}$ ), and third, the metallicity gradient is too low. For  $\beta > 1.3$ , the metallicity gradient is acceptable, but the gas distribution goes the wrong way. Besides, in the solar neighborhood, the peak of the SFR occurs after 11 Gyr since the formation of the disk, and the AMR too becomes very concave and moves outside the acceptable range. We therefore, have to make a compromise between a good fit to the data on the gas

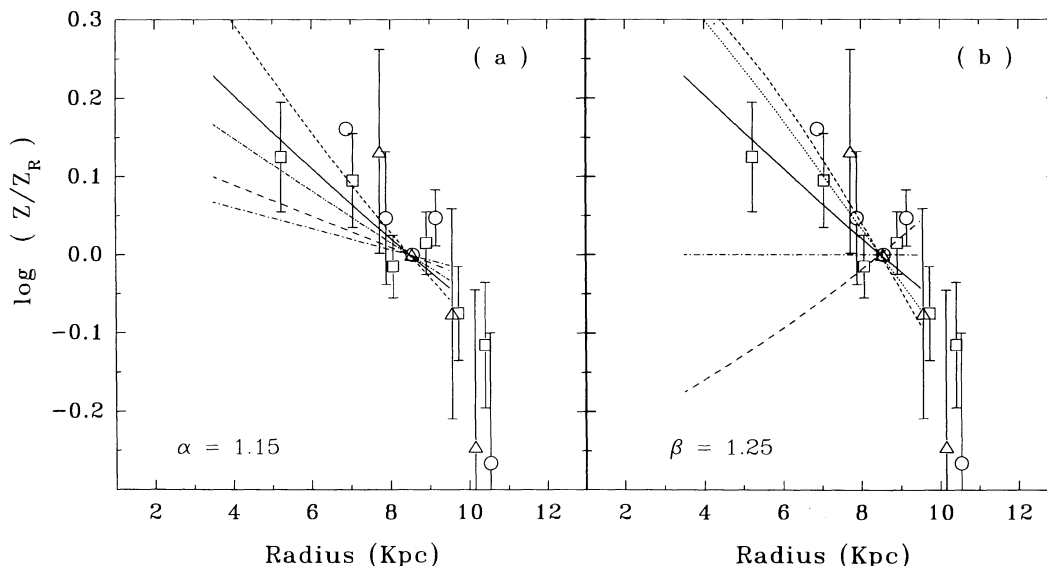


FIG. 6.—Predicted radial metallicity distribution for (a)  $\alpha = 1.15$  with different values of  $\beta$ , and (b)  $\beta = 1.25$  with different  $\alpha$ . The different types of lines correspond to the same  $\beta$  and  $\alpha$  values as in Figs. 1a and 1b, respectively. The circles are data from Cameron (1985), the triangles are from Luck (1982), and the squares are from Janes (1979).



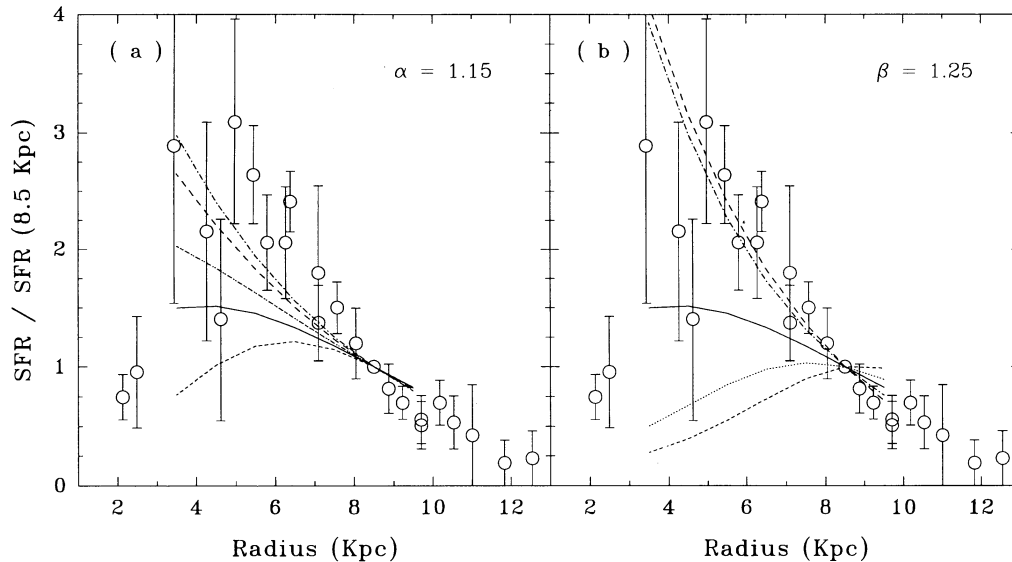


FIG. 7.—Radial distribution of the ratio of the current SFR to the current SFR at the solar neighborhood for (a)  $\alpha = 1.15$ , with  $\beta$  as in Fig. 1a, and (b)  $\beta = 1.25$ , with  $\alpha$  as in Fig. 1b.

distribution and the data on the metallicity gradient. The parameter range, which can give a reasonable fit to all the data taken together, is  $\alpha = 1.15 \pm 0.05$  and  $\beta = 1.25 \pm 0.05$ . This range of parameters also reproduces the observations on the rate of formation of white dwarfs, as can be seen from Figure 8.

#### 4.7. Can We Do Better?

As can be seen from Figures 1, 3, 4, and 8, and from Table 2, the parameter range  $\alpha = 1.15 \pm 0.05$  and  $\beta = 1.25 \pm 0.05$  gives reasonably good fits to the solar neighborhood data, but the fit to Galactic observations is at best marginal. The shape of the gas distribution and the SFR distribution cannot be reproduced. From equation (3) we see that the metallicity is inversely

proportional to the fraction of gas. Therefore, if we increase the gas mass at a given Galactocentric radius, the metallicity decreases, giving a lower gradient of metallicity.

The models assume that all solar neighborhood parameters are valid over the rest of the Galaxy. This means that the mass spectrum of the stars is a constant, which implies that the returned fraction of gas,  $R$ , and the yield  $y$  are the same all over the Galaxy. We have also assumed that the constant of proportionality in the expression for the SFR (see eq. [1]), which is in a way a measure of the efficiency of star formation is the same all over the Galaxy. If we want that the models reproduce the gas density at each Galactocentric radius, we will have to relax one of these conditions, that is, either allow the mass spectrum to vary, which will also mean the variation of  $R$  and  $y$ , or let the efficiency of star formation vary.

Whether the IMF is constant over space and time is a much debated issue. Garmany, Conti, & Chiosi (1982), from the studies of early-type star counts claimed that the high mass range of the mass spectrum showed spatial variation, but Humphreys & McElroy (1984) subsequently showed that this was a selection effect, and that the data favored a constant mass spectrum. Observations of external galaxies and globular clusters (Lequeux 1979; McClure et al. 1986; Berkhuysen 1982) do not show a large variation from the local mass spectrum. Scalo (1986) also contends that the mass spectrum is grossly the same everywhere. Therefore, significant variations in the mass spectrum may be rare, and as a first approximation we may take the IMF to be constant.

We have, therefore, allowed the constant of proportionality  $a$ , in equation (1) to vary across the Galaxy to see whether we can reproduce the gas distribution. We find that the variation required is quite small, the required value of  $a$  between 3 to 10 kpc of the Galactic center is within 10% of its value at the solar neighborhood. We must bear in mind that the relative uncertainty in the observed gas mass density distribution is quite high. The resulting distribution of metallicity and SFR across the face of the Galaxy is shown in Figure 9. We find that the fit to the SFR distribution improves considerably, and the predicted metallicity distribution shows signs of steepening

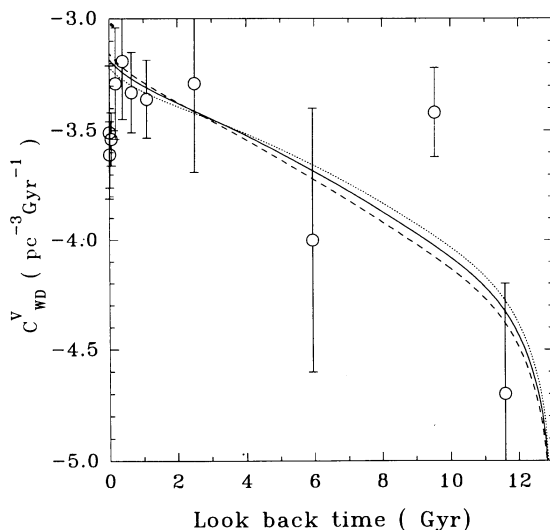


FIG. 8.—Predicted rate of the formation of white dwarfs in the solar neighborhood for the adopted range of parameters. The data are from Rana (1990). The solid curve is for the model with  $\alpha = 1.15$  and  $\beta = 1.25$ , the dotted curve is for the model with  $\alpha = 1.10$ ,  $\beta = 1.30$ , and the dashes represent the model with  $\alpha = 1.10$ ,  $\beta = 1.20$ .

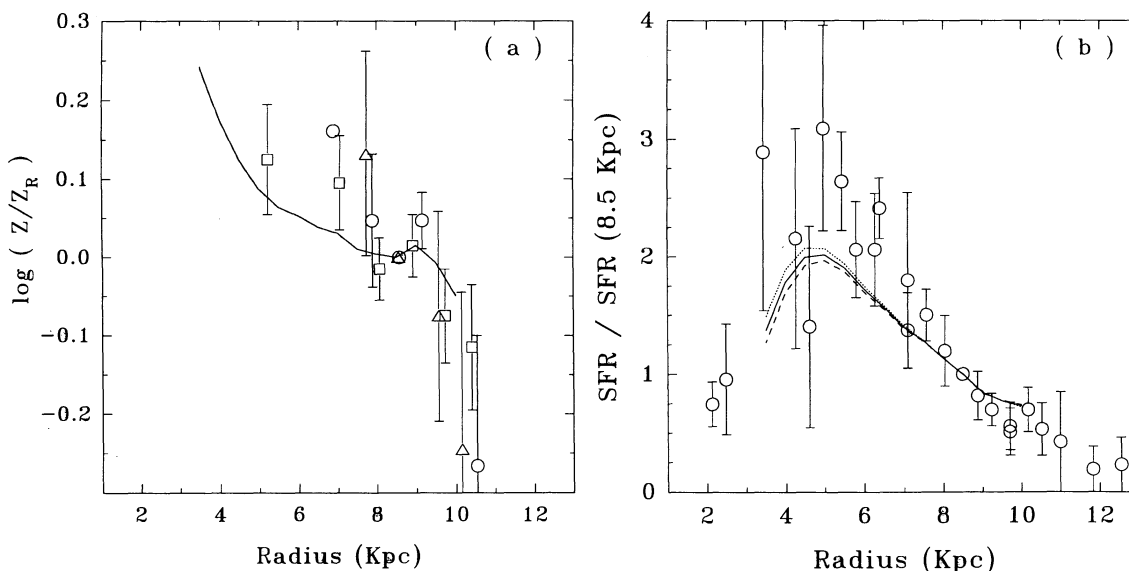


FIG. 9.—(a) Radial distribution of metallicity if the constant of proportionality in the expression for the star-formation rate is allowed to vary at each radius in order to reproduce the surface density of gas. (b) The radial distribution of the present star-formation rate for the same variation. The solid curve is for  $\alpha = 1.15$ ,  $\beta = 1.25$ , and the dashed curve is for  $\alpha = 1.20$ ,  $\beta = 1.20$ . The dotted curve is for  $\alpha = 1.10$ ,  $\beta = 1.30$ .

beyond the solar neighborhood, the way observations suggest. One must note that the variation in the value of  $a$  across the face of the Galaxy does not in any way change the predictions of the models at the solar neighborhood. Table 3 tabulates the variation of the constant of proportionality as a function of the Galactocentric radius  $R_G$ .

The fact that to reproduce the gas distribution and the metallicity gradient we do not need to depend on the parameters  $\alpha$  and  $\beta$  means that in principle, the acceptable range of the two parameters can be larger. However this does not happen. The constraint here is the radial distribution of the SFR. For small values of  $\alpha$ , a uniform constant of proportionality produces more gas at given radius than is observed. This would mean, that in order to be able to reproduce the gas distribution, the star-formation efficiency would have to be somewhat greater than that at the solar neighborhood. This in turn would mean an increase in the SFR, but the SFR relative to the solar neighborhood actually decreases due to the lower dependence on gas density. Better results are achieved by increasing the value of  $\beta$ , but then the SFR and the AMR would no longer fit the solar neighborhood data. For larger values of  $\alpha$ , we can have large values of  $\beta$  which satisfy the solar neighborhood constraints (Paper I). In that case, however, the

predicted gas mass is somewhat less than that observed, and to correct for this the constant of proportionality has to be decreased. This causes a decrease in the relative SFR despite an increase in the dependence of the SFR on both the gas density and the metallicity. Thus the acceptable range of parameters does not change.

#### 4.8. Is the Star-Formation Rate Related to Molecular Hydrogen?

It has been claimed by Rana & Wilkinson (1986) that the star formation in the Galaxy as well as external galaxies has a better correlation with the surface density of molecular hydrogen rather than with the surface density of atomic hydrogen or that of the total gas, and they claim that

$$\psi \propto \Sigma_{\text{H}_2}^k. \quad (4)$$

They had postulated that the dependence of the surface density of  $\text{H}_2$ ,  $\Sigma_{\text{H}_2}$ , on the surface density of gas,  $\Sigma_g$  has the form

$$\Sigma_{\text{H}_2} \propto \Sigma_g Z_{16}^b, \quad (5)$$

where,  $Z_{16}$  is the abundance of oxygen.

We have considered an SFR which depends on the abundance of iron rather than oxygen. In order to see if this form, with the acceptable range of parameters that emerges, is still proportional to the surface density of molecular hydrogen, we have plotted the logarithm of the fraction of molecular hydrogen as a function of  $(Z/Z_R)$ , for each set of metallicity data mentioned in § 2. The power  $b$  in equation (5) would correspond to the ratio  $(\alpha/\beta)$  in our case. From Figure 10a we can see that the ratio of the powers we obtain is consistent with observations. From Figure 10b we see that the SFR also reproduces the distribution of molecular hydrogen in the Galaxy reasonably well. Thus we can claim that the form of the SFR adopted in the present work, with  $\alpha = 1.15 \pm 0.05$ ,  $\beta = 1.25 \pm 0.05$ , is consistent with a star formation rate which is proportional to the surface density of molecular hydrogen, with  $b = 1.3 \pm 0.3$  (Rana & Wilkinson 1986, 1988).

TABLE 3

THE VARIATION OF "a," THE CONSTANT OF PROPORTIONALITY IN EQUATION (1), WITH GALACTOCENTRIC RADIUS

GALACTOCENTRIC RADIUS (kpc)	"a" FOR MODELS WITH		
	$\alpha = 1.10$ $\beta = 1.30$	$\alpha = 1.15$ $\beta = 1.25$	$\alpha = 1.20$ $\beta = 1.20$
3.50	0.360	0.290	0.235
4.50	0.340	0.272	0.220
5.50	0.334	0.269	0.218
6.50	0.336	0.274	0.224
7.50	0.337	0.278	0.230
8.50	0.344	0.286	0.240
9.50	0.351	0.296	0.251

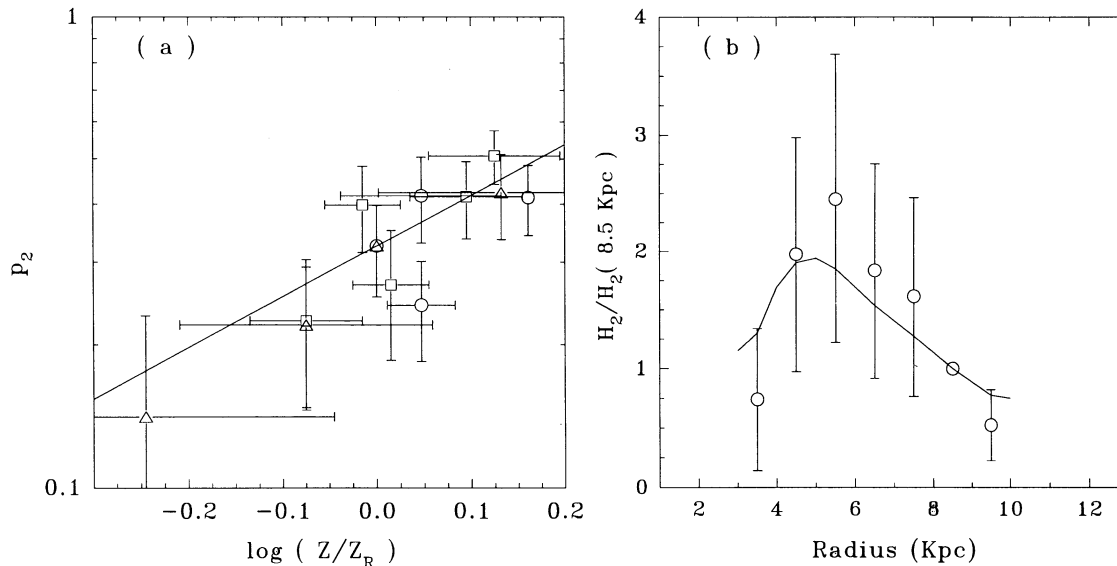


FIG. 10.—(a) Ratio of the surface mass density of molecular hydrogen to that of the total amount of gas— $p_2$ —plotted as a function of iron abundance normalized to the abundance at the solar neighborhood. The circles are metallicity data from Cameron (1985), triangles from Luck (1982) and squares from Janes (1979). The solid line is the relationship predicted from the adopted SFR with  $\alpha = 1.15$ , and  $\beta = 1.25$ , and the  $H_2$  mass parameterized as in eq. (5), but with  $Z$  representing the abundance of iron instead of oxygen. (b) Predicted radial distribution of  $H_2$  for the SFR with  $\alpha = 1.15$  and  $\beta = 1.25$ .

#### 4.9. Will Relaxing the Instantaneous Recycling Approximation Change the Conclusions?

Since a fairly large fraction of iron is produced by intermediate-mass stars in Type Ia supernovae, it becomes necessary to ask whether the results we have stated will hold once IRA is relaxed. In order to test this we relaxed IRA for some values of the parameters to see to what extent the results would change. We find that the results are consistent provided the supernova mass limits considered are the same as those obtained from the IMF. However to combat the slow rise in metallicity at early epochs, an insignificantly higher initial

metallicity has to be assumed ( $[\text{Fe}/\text{H}] = -0.84$  dex instead of  $-0.85$  dex). We had obtained similar results in Paper I. Figure 11 shows the results of relaxing IRA for a few selected sets of parameters. We show the IRA results for comparison. We see that the difference in results is not enough to change any of the conclusions we have drawn in the previous sections.

#### 5. CONCLUSIONS

We have tested closed models of Galactic chemical evolution with star-formation rates of the form  $\psi \propto \Sigma_g^\alpha Z^\beta$ . We find that this simple model with only two free parameters gives reason-

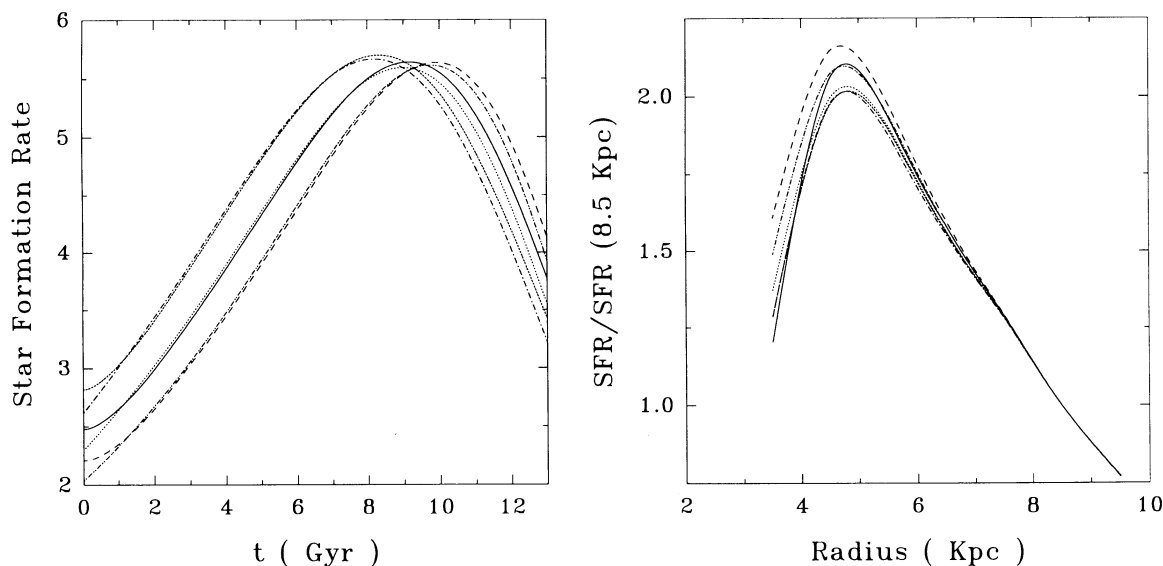


FIG. 11.—History of the star-formation rate when instantaneous recycling approximation is relaxed. The long-dashed curve is for the SFR with  $\alpha = 1.10$ ,  $\beta = 1.30$ , with the corresponding curve with instantaneous recycling assumed shown as the chain dotted curve. The solid curve is the SFR with  $\alpha = 1.15$ ,  $\beta = 1.25$ , the corresponding SFR with IRA is shown as the dotted curve. The short-dashed and dot-dashed lines are, respectively, the SFRs without and with IRA for  $\alpha = 1.20$ ,  $\beta = 1.20$ . (b) Radial distribution of the star-formation rate normalized to 1 at the solar neighborhood. The different curves correspond to the same models as in (a).

able fits to all observational constraints they have been tested against. The two parameters too are well constrained. The result is all the more surprising simply because more complex multiparameter models are generally not expected to do much better in terms of fitting *all* the relevant observations. We reach the following conclusions from our study:

1. The adopted form of the SFR can fit the history of star formation in the solar neighborhood as derived by Soderblom et al. (1991) from chromospheric ages of stars. The SFR thus derived is nearly constant. The ratio of the past average to the present SFR is around  $1.2 \pm 0.3$ . The model gives a good fit to the G dwarf metallicity distribution function for an initial metallicity of  $-0.85$  dex.

2. It is important to derive the initial mass function from the present day mass function for each SFR. The history of the SFR determines the IMF, and hence influences quantities like the total surface mass density, returned fraction, yield, and the current SFR, which are derived from the IMF.

For the adopted range of parameters, the total surface mass density is around  $51_{-9}^{+15} M_{\odot} \text{pc}^{-2}$ . This result is consistent with dynamical estimates of the surface mass density of total mass, which range from  $54 \pm 8 M_{\odot} \text{pc}^{-2}$  (Gould 1990) to  $48 \pm 8 M_{\odot} \text{pc}^{-2}$  (Kuijken & Gilmore 1991). Thus we see that we do not have to postulate any form of non-baryonic dark matter in the local disk.

The returned fraction of gas is around 0.207, and the present star-formation rate is  $3.54 M_{\odot} \text{pc}^{-2} \text{Gyr}^{-1}$ .

3. For  $\alpha = 1.15 \pm 0.05$  and  $\beta = 1.25 \pm 0.05$ , the models give very good fits to the solar neighborhood data. The required yield of iron is about  $0.574(Z_{\odot})_{\text{Fe}}$ , which can be matched with that obtained from the IMF if the mass range of the progenitors of Type II supernovae is taken to be around  $9.5 \pm 1.0 M_{\odot}$  to  $50 M_{\odot}$ . The match with the Galactic data however, is marginal.

4. Much better fits to the Galactic data can be obtained if the constant of proportionality in the expression of the star-formation rate is allowed to vary across the face of the Galaxy. In the above range of parameters, the variation required is not very large, and the constant is within 10% of that at the solar neighborhood. Surprisingly, this required variation is very small compared to the uncertainty in the estimates of the gas surface density. The value of  $a$  ranges from  $0.290 \text{Gyr}^{-1}(M_{\odot} \text{pc}^{-2})^{-0.15} Z_{\odot}^{-1.25}$  at  $R_G = 3.5$  kpc to  $0.296 \text{Gyr}^{-1}(M_{\odot} \text{pc}^{-2})^{-0.15} Z_{\odot}^{-1.25}$  at  $R_G = 9.5$  kpc for  $\alpha = 1.15, \beta = 1.25$ .

5. The form of the SFR with the parameters in the allowed range is consistent with one which is proportional to some power of the surface density of molecular hydrogen. The adopted form of the SFR is able to reproduce the Galactic distribution of  $\text{H}_2$ .

We thank the anonymous referee for useful comments and suggestions.

#### REFERENCES

- Amendt, P., & Cuddeford, P. 1991, *ApJ*, 368, 79  
 Bahcall, J. N., Schmidt, M., & Soneira, R. M. 1983, *ApJ*, 265, 730  
 Basu, S., & Rana, N. C. 1992, *ApJ*, 393, 373  
 Becker, S. A., & Iben, I. 1980, *ApJ*, 237, 111  
 Berkhuizen, E. 1982, *A&A*, 112, 369  
 Bhat, C. L., Houston, B. P., Issa, M. R., Mayer, C. J., & Wolfendale, A. W. 1985, *Nature*, 314, 511  
 Branch, D. 1984, in *Stellar Nucleosynthesis*, ed. C. Chiosi & A. Renzini (Dordrecht: Reidel), 19  
 Bronfman, L., Cohen, R. S., Alvarez, H., May, J., & Thaddeus, P. 1988, *ApJ*, 324, 248  
 Burton, W. B., & Gordon, M. A. 1978, *A&A*, 63, 7  
 Cameron, L. N. 1985, *A&A*, 147, 47  
 Carlberg, R. G., Dawson, P. C., Hsu, T., & Vandenberg, D. A. 1985, *ApJ*, 294, 674  
 Deul, E. R. 1988, Ph.D. thesis, Univ. Lieden  
 Evans, R., van den Bergh, S., & McClure, R. D. 1989, *ApJ*, 345, 752  
 Garmany, C. D., Conti, P. S., & Chiosi, C. 1982, *ApJ*, 263, 777  
 Gould, A. 1990, *MNRAS*, 244, 25  
 Guibert, J., Lequeux, J., & Viallefond, F. 1978, *A&A*, 68, 1  
 Humphreys, R. M., & McElroy, D. B. 1984, *ApJ*, 367, L9  
 Janes, K. A. 1979, *ApJS*, 39, 135  
 Kuijken, K., & Gilmore, G. 1991, *ApJ*, 367, L9  
 Lacey, G., & Fall, S. M. 1985, *ApJ*, 290, 154  
 Lequeux, J. 1979, *A&A*, 71, 1  
 Luck, R. E. 1982, *ApJ*, 256, 177  
 Lyne, A. G., Manchester, R. N., & Taylor, J. H. 1984, *MNRAS*, 213, 613  
 Maeder, A., & Meynet, G. 1989, *A&A*, 210, 155  
 McClure, R. D., et al. 1986, *ApJ*, 307, L7  
 Mezger, P. G. 1978, *A&A*, 70, 565  
 Meusinger, H., Reimann, H.-G., & Stecklum, B. 1991, *A&A*, 245, 57  
 Miller, G. E., & Scalo, J. M. 1979, *ApJS*, 41, 513  
 Narayan, R. 1986, in *IAU Symp. 125, The Origin and Evolution of Neutron Stars*, ed. D. J. Helfand (Dordrecht: Reidel), 67  
 Nomoto, K. 1984, *ApJ*, 277, 791  
 Nomoto, K., Shigeyama, T., & Tsujimoto, T. 1990, in *IAU Symp. 145, Evolution of Stars: the Photospheric Abundance Connection*, ed. G. Michaud (Dordrecht: Reidel) 21  
 Nomoto, K., Thielmann, F. K., & Yokoi, K. 1984, *ApJ*, 286, 641  
 Nissen, P. E. 1988, *A&A*, 199, 146  
 Nissen, P. E., Edvardsson, B., & Gustafsson, B. 1985, in *Production and Distribution of C, N, O Elements*, ed. I. J. Danziger, F. Matteucci, & K. Kj r (Garching: ESO), 131  
 Pagel, B. E. J. 1989, in *Evolutionary Phenomena in Galaxies*, ed. J. E. Beckman, & B. E. J. Pagel (Cambridge: Cambridge Univ. Press), 201  
 Rana, N. C. 1987, *A&A*, 184, 104  
 ———. 1990, *Ap&SS*, 142, 67  
 Rana, N. C., & Basu, S. 1992, *A&A*, 265, 499 (Paper I)  
 Rana, N. C., & Wilkinson, D. A. 1986, *MNRAS*, 218, 496  
 ———. 1988, *MNRAS*, 231, 509  
 Scalo, J. M. 1986, *Fund. Cosmic Phys.*, 11, 1  
 Soderblom, R. D., Duncan, D. K., & Johnson, D. R. H. 1991, *ApJ*, 375, 722  
 Sommer-Larsen, J. 1991, *MNRAS*, 249, 368  
 Strobel, A. 1991, *A&A*, 247, 35  
 Tinsley, B. M. 1980, *Fund. Cosmic Phys.*, 5, 287  
 Tosi, M., & Diaz, A. I. 1990, *MNRAS*, 246, 616  
 Twarog, B. A. 1980, *ApJ*, 242, 242  
 van den Bergh, S., McClure, R. D., & Evans, R. 1987, *ApJ*, 323, 44  
 van den Bergh, S., & Tamman, G. A. 1991, *ARA&A*, 29, 363  
 Villumsen, J. V. 1985, *ApJ*, 290, 632  
 Woosley, S. E., Weaver, T. A., & Taam, R. E. 1980, in *Type I Supernovae*, ed. J. C. Wheeler (Austin: Univ. Texas), 96